ELSEVIER

Polymer 42 (2001) 4845–4851

polymer

www.elsevier.nl/locate/polymer

Scanning electric potential microscopy imaging of polymers: electrical charge distribution in dielectrics

A. Galembeck[a], C.A.R. Costa[b], M.C.V.M. da Silva[b], E.F. Souza[c], F. Galembeck[b,*]

[a]*Instituto de Química Fundamental, Universidade Federal de Pernambuco, Pernambuco, Recife PE, Brazil*
[b]*Instituto de Química, Universidade Estadual de Campinas, Caixa Postal 6154, Unicamp, IQ, P.O. Box 6154, 13083-970 Campinas SP, Brazil*
[c]*Instituto de Ciências Biológicas e Química, Pontifícia Universidade Católica de Campinas, Campinas SP, Brazil*

Received 11 September 2000; accepted 27 November 2000

Abstract

Scanning electric potential images of polymer surfaces are presented and compared to standard non-contact AFM images. Samples used were a latex film with a well-known distribution of chemical constituents and thus of ionic electrical charges, as well as finished industrial products. Topography and electric potential images show a variable degree of correlation, thus evidencing the independence of topographic and electrical features of the samples, in the micro- and nanoscopic scales. Domains with non-zero negative or positive electric potentials are observed, extending for a few tenths of a micron and creating an electric mosaic in the otherwise neutral polymers. Large electric potential gradients are observed, e.g. in a HDPE film.

Keywords: Electric potential images; Polymer surfaces; Micro- and nanoscopic scales

1. Introduction

Polyolefins and related thermoplastics are often used as dielectrics, and this is in turn related to their strong ability to acquire static electrical charges. There are many important topics related to the problem of electrical charges within dielectrics, such as: electrets, space and residual charges, double-layer formation at interfaces and interfacial polarisation, which are shortly reviewed in the following paragraphs. There is also a relevant conceptual constraint in dealing with these problems, which is the current idea of charge neutrality as a normal state for polymer dielectrics at every relevant length scale, from the macromolecules up to the macroscopic plastic solids (films, coatings, tubes) and devices. Of course, the prevalence of electroneutrality in any physical medium suggests that the ionic species carrying opposite charges should occupy neighbouring sites and they should also move simultaneously [1].

Electrets are dielectrics with permanent electrical polarity, and they have found some important practical applications. Surface charges in electrets were measured in the early part of the twentieth century using the Lindemann electrometer, and interesting but puzzling results are already reported e.g. by Partington [2]. A recent review [3] on piezoelectric polymer electrets addresses the problem of the nature and origin of the trapped charges and their role in the stabilisation of molecular dipole orientation [4], in electrets. However, these authors exclude the possibility of polymer ionisation by accelerated electrons ejected by the electrodes, and they conclude that only the direct contact of the electrode structure to the polymer surface can lead to charge injection. The detection of gases emitted by polymers subjected to polarisation between electrodes showed the formation of $C_2H_4^+$, which is a strong indirect evidence for transient polymer macro-ion formation, but direct evidence for the existence of macro-ions has not been obtained.

In another review article, on the non-linear optical polymer electrets, the authors acknowledge that a corona discharge produces and carries chemically active species which tend to attack and modify the surface and subsurface layers of organic materials, but the spatial distribution and chemical identity of the resulting charge species responsible for polymer polarisation is not described [5]. The high stability of electret charge is predicted by a theory involving a competition between the rate of current–carrier creation in activation processes and the rate of annihilation due to recombination and carrier capturing on the electrodes as well as by free, implanted charge already present in electrets [6]. The existence of ionic carriers is considered, but these are not identified, in this work.

* Corresponding author. Tel.: +55-19-289-3118; fax: +55-19-788-3023.
E-mail address: fernagal@iqm.unicamp.br (F. Galembeck).

0032-3861/01/$ - see front matter
PII: S0032-3861(00)00921-6

In his recent text on dielectrics, Robert [7] emphasises that the electrical polarisation of a dielectric has four components. Three of these (orientation, atomic and electronic) are well-known and they are acknowledged in basic texts treating the electrical polarisation of matter. However, Robert also calls attention to the interfacial polarisation, the result of local accumulations of charges due to the migration phenomena, and concentrated around imperfections such as impurities, vacancies, grain boundaries and others. The interfacial polarisation may take several minutes to build up, and the detailed nature of the mobile charges is not described by this author. The current difficulties for the fundamental understanding of electrically charged entities within dielectrics are summed up by this author, in the "almost total impossibility of using models based on fundamental theories" to understand partial discharges phenomena. Of course, these difficulties have not prevented the use of thermally stimulated discharge currents in polymers, in the study of polymer relaxation [8–10].

The formation of double-layers of opposite electrical charges by two dielectric contacting phases was recognised by Skinner and other authors [11,12], and the existence of a double layer at the polymer–metal interface was proven by Possart and Roder [13]. Derjaguin [14] assigned to the corresponding electrostatic attraction an essential role in adhesion. Later on, the electrostatic component of adhesion was determined quantitatively by two groups, and the values obtained indicate that it amounts to a few percent only of the actual work of adhesion. For this reason, the electrostatic contribution to adhesion does not receive great attention, currently [15].

Indeed, the formation of an electrical double layer at an interface is expected, considering the differences of dielectric constant between the two adjoining phases. Since most crystalline polymers are indeed multiphase systems, they should intrinsically display internal charge separation. This idea is supported by evidence showing that the crystalline–amorphous interface plays an important role not only as a charge trapping site but also in carrying an important amount of the total polarisation in PVDF. The differences in dielectric constants of e.g. monocrystalline and amorphous polyethylene (and other partially crystalline thermoplastics) are probably small, but their electronic polarisation component is sufficient to impair the transparency of the partially crystalline polymer.

Beyond the differences of dielectric constant between amorphous and crystalline polymer domains, there are other factors for the formation of differentiated domains within a polymer: oxidised polymer can be segregated, as well as the immiscible catalyst residues and contaminants introduced during fabrication of polymer and artefacts.

An important topic concerning electrical polarisation in dielectrics are the space charges. These and injection effects in bulk polymer were examined in detail, due to their relevance for electrical ageing of extruded dielectric cables [16]. The concept of a critical field above which charge injection [17] occurs is in agreement with the observation that below 1.6×10^7 V/m there is no charge injection in XLPE. PE has a dark non-ohmic conductivity [18] and it is electroluminescent under large electrical fields. However, little is known on the nature of the chemical entities bearing the electrical charges associated to these phenomena as well as on their spatial distribution throughout the polymer bulk and surface. Great efforts have been done to develop adequate theories and phenomenological relations between conduction activation energies, electric field, pressure [19] and other variables.

Following Crine [20], mechanical and electromechanical stresses induce the formation of sub-microcavities within the polymer. Electrons can then move without scattering within the sub-microcavities and this may lead to further degradation. Detection of electroluminescence in PE [21] subjected to high fields is an evidence for the formation of chemical species in high-energy states, and some among these are probably trapped within the inert polyolefin; but they have not been identified or mapped. This is remarkable, because the formation of free radicals and end-groups of scission molecules formed in polyethylene, polypropylene and polycaprolactam under axial tension was already investigated many years ago, and their association with submicrocrack generation in stressed polymers was well established [22]. In this work, Zhurkov and colleagues found that the number of scission chains is as large as 10^{19} cm^{-3}, approximately three orders of magnitude larger than the number of free radicals detected in the stressed polymer, which is in turn about of the same order of magnitude as the detected sub-microcracks. This raises the possibility of formation of significant amounts of carbon and oxygen anions and cations following polymer stressing, which would then be trapped in the dielectric.

Free radicals are conveniently identified even at very small amounts by electron spin resonance (ESR), but the same is not true for macrocations and anions, due to the non-existence of a suitable experimental technique. This is also evidenced by the studies on ion beam effects in polymer films: polymer conductivity increases by as much as 10^{15} in ion beam-implanted polymers, and there is rather detailed information on depth distribution of the implanted species as well as on free-radical formation. However, the existence of polymer-derived ionic species is not considered, and the conductivity changes are assigned to the formation of carbonisation as well as to an associated degenerated quasi-two-dimensional electron gas [23].

Direct measurement of electric potentials in dielectrics is a difficult task, although techniques have been available during the twentieth century. On the other hand, specific techniques have been devised in the case of monolayers formed by organic substances (e.g. surfactants, polymers) on top of aqueous solutions: the radioactive electrode and the oscillating electrode technique revealed a great deal of information on the distribution and orientation of different substances on liquid surfaces [24].

More recently, the advent of the scanning probe microscopes made techniques available for sensing charges, dielectric constants, film thickness of insulating layers, photovoltage and electric potentials [25] and ferroelectric domain imaging [26]. For instance, the electrostatic force microscope (EFM) maps the spatial variation and potential energy difference between a tip and a sample, which results from non-uniform charge distributions and variations in surface work function [27]. A tapping mode AFM coupled to electrostatic force modulation was used to image a polystyrene latex layer deposited on silicon, showing a large and intriguing contrast between neighbouring latex particles [28]. The detection of localised charges on polymers was demonstrated by Terris et al. [29], using PMMA samples with implanted charges. We have used the scanning electric potential microscopy (SEPM), proceeding in a way similar to these authors for the examination of polymer surfaces, and we obtained a wealth of information, well beyond what is obtained using the more usual atomic force (AFM) techniques, either contact, non-contact, lateral force, intermittent contact and so on.

In this work, we report SEPM images of polymers. The samples used are both model systems as well as technical products.

2. Experimental

2.1. SEPM

AFM and SEPM images were acquired using a Topometrix Discoverer instrument. SEPM in this instrument uses the standard non-contact AFM set-up, but with the following modifications: the Pt-coated conducting tip is fed with an AC signal, 10 kHz below the frequency of the normal AFM oscillator, which matches the natural frequency of mechanical oscillation of the cantilever-tip system (40–70 kHz). During a measurement, the mechanical oscillation of the tip is tracked by the four-quadrant photodetector and analysed by two feedback loops. The first loop is used in the conventional way to control the distance between tip and sample surface, while scanning the sample at constant oscillation amplitude. The second loop is used to minimise the electric field between tip and sample: a second lock-in amplifier measures the tip vibration at the AC frequency oscillation while scanning, and adds a DC bias to the tip, to recover the undisturbed AC oscillation. This technique differs from that used by Terris, who measures the phase displacement of the AC voltage, while in the Topometrix set up we cancel the phase displacement by DC biasing. The image is built using the DC voltage fed to the tip, at every pixel, thus detecting electric potential gradients throughout the scanned area. This technique is reminiscent of the oscillating electrode technique for monolayer study: both use an oscillating electrode separated from the sample by an air gap. The major difference between both techniques is the detection technique used, since SEPM uses a phase detection of the voltage applied.

Image processing was performed in an IBM PC microcomputer using the Image-Pro Plus 4.0 (Media Cybernetics) or the Topometrix image analyser program.

2.2. Sample preparation

Poly(styrene-*co*-hydroxyethylmetacrylate), PS-HEMA, was prepared in this laboratory. Its elemental distribution maps were obtained using a powerful analytical technique, energy loss imaging in the transmission electron microscope (ELSI-TEM) [30,31]. Following these previous results, the dry particles have a negatively charged core and a positively charged shell. The negative charges are due to the sulphate residues attached to the polymer chains, which are more concentrated in the inner part of the (dry) latex particles than in the outer shell. On the other hand, the potassium counter-ions cluster at the particle outer layers, making a narrow shell, with excess positive charge.

Low density polyethylene, high-density polyethylene and polypropylene were commercial samples supplied by

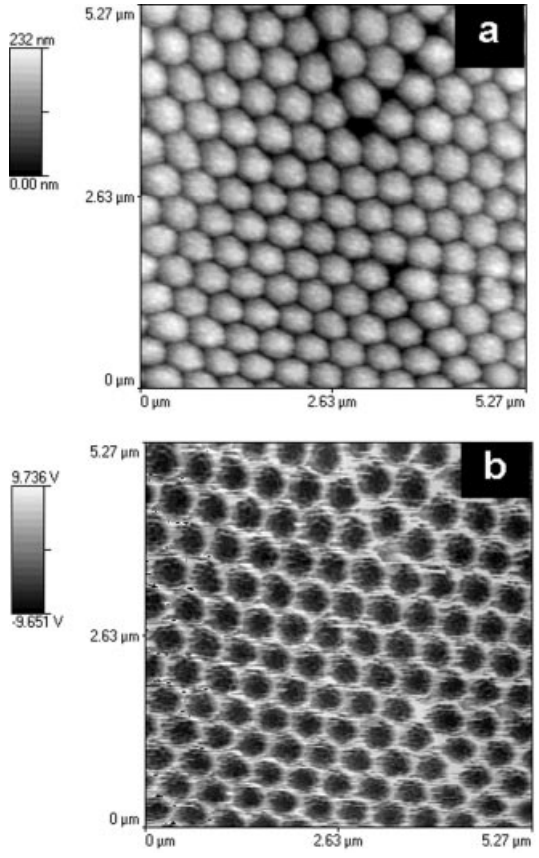

Fig. 1. AFM (upper) and SEPM (lower) images of a self-assembled poly (styrene-*co*-hydroxyethylmetacrylate) latex macrocrystal. Particles have a "raspberry" morphology, and according to EELS microanalysis the negatively charged sulphate groups are in the interior of the particles, and the potassium counter-ions are clustered at the particle surfaces, according to Refs. [30,31].

Poliolefinas. Before use, the polyolefin films were washed with water and ethanol, and air-dried. Polymers identity was verified by IR spectra and X-ray diffraction.

The samples were mounted in the appropriate sample holders, supplied by Topometrix.

3. Results

A core and shell latex: PS-HEMA. AFM topography and SEPM images of a film of this latex are in Fig. 1. The SEPM image shows that the tip was positively biased over the particle outer layers, relative to the particle centres. This result is expected from the ELSI-TEM results, showing that the sulphate initiator residues are distributed throughout the particles, while the potassium counter-ions are in a particle outer shell. The qualitative features of the SEPM image are thus validated by the former ESI-TEM data, which are completely independent from the present results.

Low-density polyethylene. Topography and SEPM images of a PEBD sample are in Fig. 2. In this case, it was not possible to obtain a SEPM image of the clean dry film. However, an image was obtained after wetting the film with an aqueous solution of the

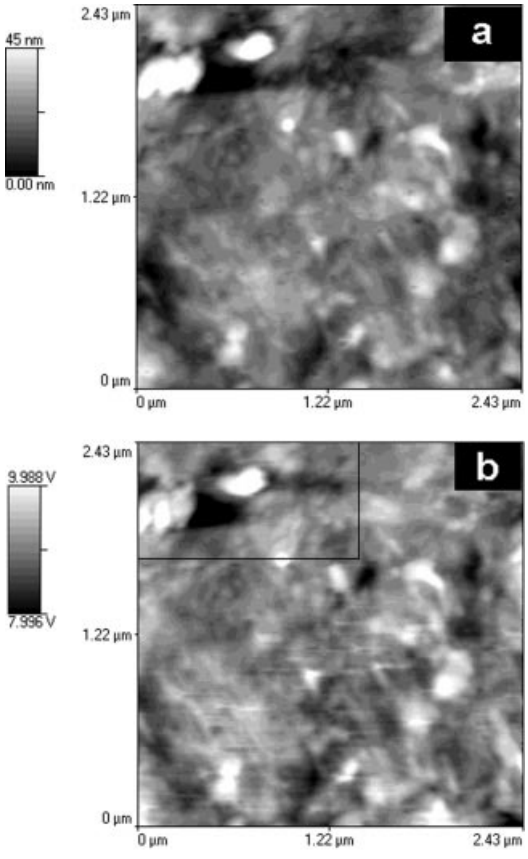

Fig. 2. AFM and SEPM images of a low-density polyethylene film (Poliolefinas grade 301).

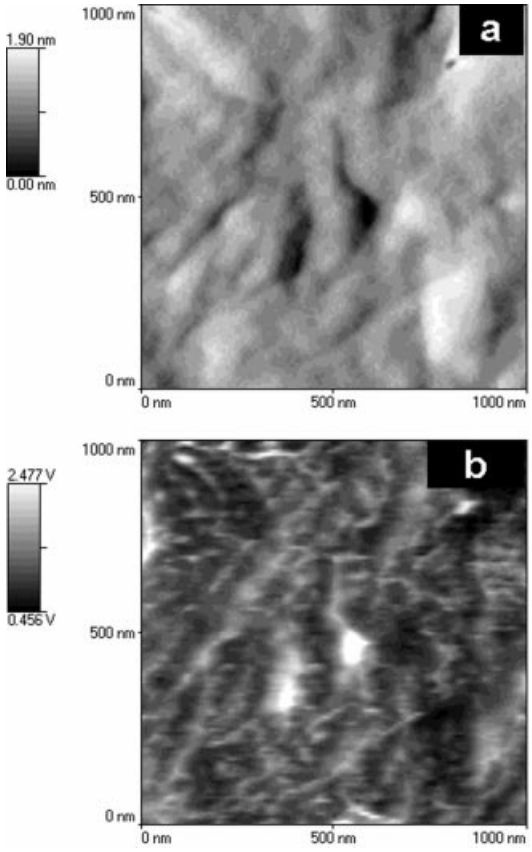

Fig. 3. AFM and SEPM images of another low-density polyethylene film (poliolefinas grade 687).

non-ionic surfactant Renex 80 (1%, added to 10^{-4} M KCl) and wiping it with lintless tissue paper. The two images are very similar, which may suggest that the Van der Waals forces dominate both. However, a closer examination reveals a mismatch between them, e.g. in the areas enclosed by a rectangle in the upper left corner. We conclude that in this film there is some correlation between the accumulation of charge-bearing entities and the topography features. Most often, the elevations contain an excess of positive electric charges (or a deficiency of negative charges), relative to surface depressions.

However, in another PEBD sample the result obtained is quite different: the topography of sampled area displays depressions and elevations (see Fig. 3), and the SEPM image shows sharp line features with a positive potential relative to neighbouring broader domains. As opposed to the previous case, in this sample the topography depressions are positive, relative to elevations. In another scan of an area of this sample (Fig. 4), the tip was allowed to scratch the surface, creating damaged areas. These damaged areas appear very bright in the SEPM image, thus corresponding to the more positive potentials observed in this sample. This is interesting, because the depressions created by

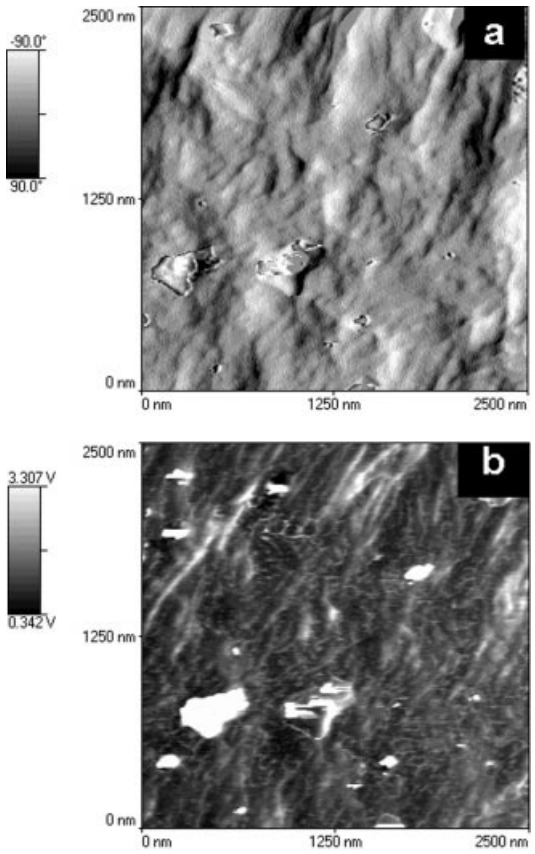

Fig. 4. AFM and SEPM images of a scratched low-density polyethylene film, showing scratched areas.

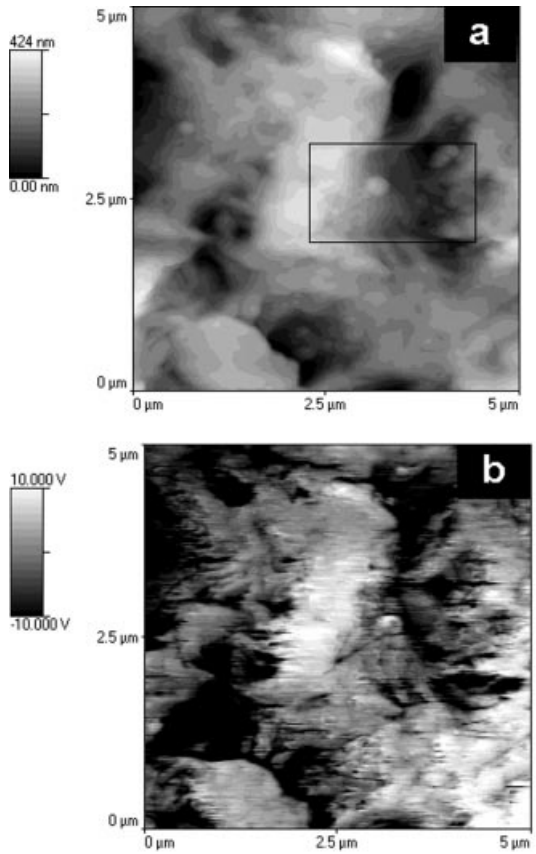

Fig. 5. AFM and SEPM images of a high-density polyethylene film.

scratching acquire the same potential sign as the pre-existing depressions.

High-density polyethylene. Images of a high-density polyethylene film are in Fig. 5. In this case, the SEPM contrast obtained is very high, and both the upper and lower limits of the bias voltage scale were reached in a large number of pixels, which means that some parts of the image are saturated and thus "flattened". Generally speaking, the surface protuberances appear as more negative than the depressions, but there are some areas in which this type of correlation is not observed (marked with a rectangle, in Fig. 5).

Polypropylene film. The AFM image of this sample displays sharp elevations with elliptical or quasi-spherical shapes, dispersed throughout a smoother background, as seen in Fig. 6. In the SEPM image there are features corresponding to the elevations, but these appear as dark spots surrounded by bright rings. Consequently, the elevations have a core-and-shell structure, with a negative core and a positive shell, dispersed throughout a background with detectable charge density fluctuations.

Polypropylene plate. Acquisition of images of a thick PP plate was very easy, and the SEPM contrast is almost coincident with the topography image (see Fig. 7).

4. Discussion

The contrast observed in the image of the model latex can be easily understood, considering the known microchemical features of this system. When the tip scans the adjacent particle sides, it senses a domain of excess positive charge (due to the accumulation of potassium counter-ions), as opposed to the particle centres. This is reflected in the biasing of the tip, used to build the SEPM image and it shows that the information contained in the SEPM image can be understood, at least concerning the relative electrical characteristics of neighbouring areas.

The SEPM images of the various PE and PP samples examined reveal interesting features, with variable degrees of correlation with the topography image. This variability in the correlation between the two imaging modes is reassuring: on one hand, the lack of correlation observed in some cases shows that these images are formed by independent (geometric and electric) characteristics of the sample. On the other hand, the good correlation observed in other cases may be understood considering that the protruding sites have both a chemical and electrical nature differentiated from their neighbours.

There are cases of correlated images (e.g. Figs. 5 and 7), in which the SEPM image contrast is sharper than can be explained by the topography; in this respect, SEPM shows a

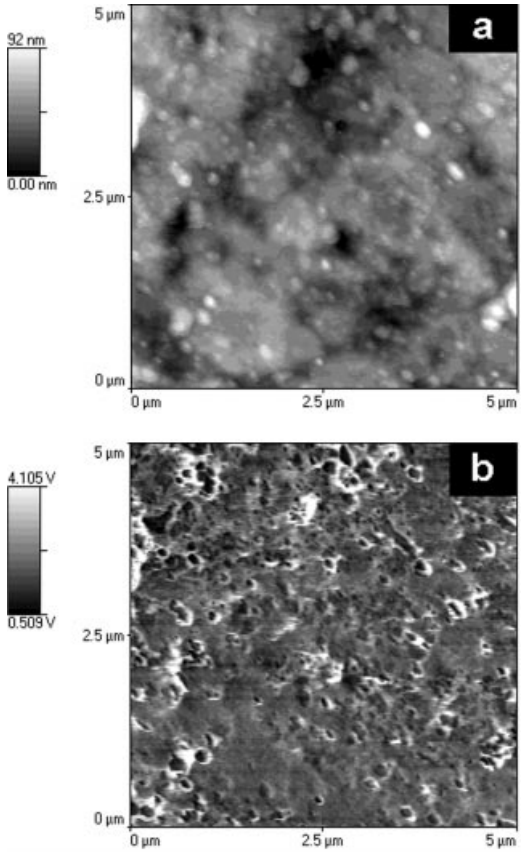

Fig. 6. AFM and SEPM images of a thin polypropylene film.

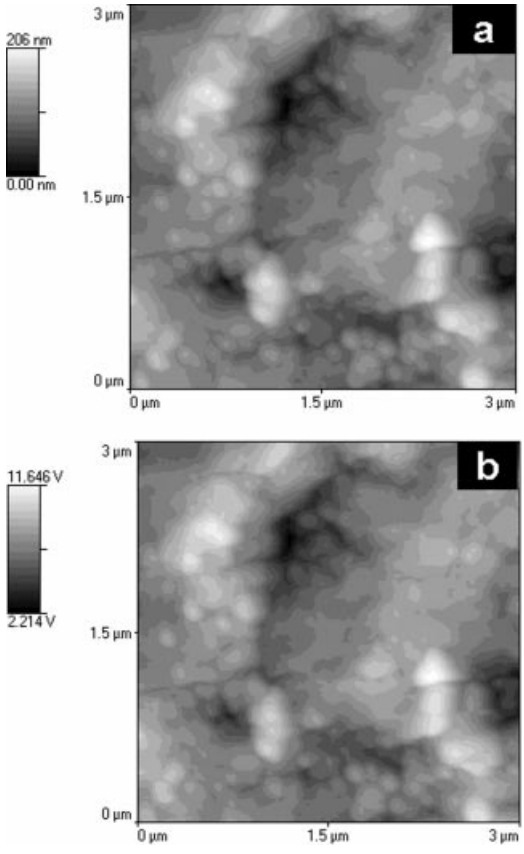

Fig. 7. AFM and SEPM images of a 5 mm-thick polypropylene sheet.

potential for revealing sample features not shown by normal AFM images.

The electric contrast in the PE and PP samples is not easily understood, considering current knowledge on electric charges in thermoplastics, which was addressed in the introduction section of this paper. It may be assigned to different factors, such as:

1. polymer oxidation, with the corresponding accumulation of polar material at some points in the polymer surface, thus creating sites with different work functions, thus allowing for electron transfer from one to another site;
2. accumulation of catalyst residues, or of residues of processing agents used in plastic transformation.

The elucidation of the relevant factors will depend on our ability to acquire microchemical information on the electrically contrasting domains in the thermoplastic polymers. If this is successfully done (e.g. by ESI-TEM or Raman microspectrophotometry), it will allow us to progress into identifying the chemical groups responsible for the observed electrical features.

An intriguing consequence of these images is the detection of sharp electric potential gradients in the polymer surfaces. For instance, in the PP thin film there are potential differences of a few volts, across distances smaller than 100 nanometers. This corresponds to electric potential gradients in excess of 10^5 V/cm throughout the film, which is probably quite significant for its mechanical, optical and electrical properties.

In their recent work, Wu and colleagues [1] examined hydronium ions deposited at a methylpentane–water interface, and they showed that the migration of the ions into the hydrocarbon is strongly dependent on the amount of water contacting the interface. Charge clusters may be formed at interfaces, and they are partitioned according to the nature of the contacting phases. Martin and co-workers [32] observed in an earlier work that the force on a tip scanning over a photoresist film was much more irregular than when the tip scanned the silicon wafer under the resist. We can now suggest an explanation for this observation, as follows: electrically differentiated domains in the resist are responsible for the enhanced contrast imparted by the resist to the wafer image.

The result obtained with LDPE 687, in which the film surface was scratched (see Fig. 4) shows the possibility for the observation of a sample beneath its surface (but perhaps at the cost of damaging a probe tip). In this case, there seems to be not only horizontal electric potential gradients, but also a vertical gradient, in which the subsurface is much more positive than the surface layer. However, we have also to consider the

possibility for tribochemical [33] charge deposition at the damaged areas.

As in all other cases of SPM imaging, the interpretation of these images is not straightforward, and it will depend on the progress in image calculation. Modelling of non-contact scanning force microscopy on ionic surfaces and image calculation combining the effects of Van der Waals and electrostatic interactions has been done recently but in very simple cases, and this will probably help in the interpretation of the experimental images, in the near future [34].

To conclude, the results presented in this work reveal a rich pattern of electric potential contrast in rather usual thermoplastic insulators. This is interesting from two points of view: first, an additional technique is available for polymer surface imaging, contributing with hitherto unavailable information; and second, this may contribute relevant information on the electrical properties of these materials, as well as on the nature of the charge-bearing species and their role on insulator stability [35].

5. Conclusions

SEPM images of polymers yield information on electrical potential distribution across the polymer surfaces. SEPM images are different from topography images in some cases, but they are correlated in others. There are domains of different electrical characteristics in polymers, extending for nanometers to micron lengths. Polymer electroneutrality is thus a result of charge balance but in a supramolecular or colloidal size scale, not necessarily in the size scale of micro- or macromolecular ion pairs or ion clusters.

Acknowledgements

F.G. acknowledges grants from Fapesp, Pronex/Finep/MCT and CNPq.

References

[1] Wu K, Iedema MJ, Cowin JP. Science 1999;286(5449):2482–5.
[2] Partington JR. An advanced treatise on physical chemistry, vol. 5. London: Longmans, 1966. p. 356.
[3] Eberle G, Schmidt H, Eisenmenger W. IEEE Trans Dielectr Electr Insul 1996;3(5):624–46.
[4] Bihler E, Holdik K, Eisenmenger W. IEEE Trans Electr Insul 1987;22(2):207–10.
[5] Bauer-Gogonea S, Gerhard-Multhaupt R. IEEE Trans Dielectr Electr Insul 1996;3(5):677–705.
[6] Malecki JA. Phys Rev B 1999;59(15):9954–60.
[7] Robert P. Electrical and magnetic properties of materials. Norwood: Artech House, 1988. p. 300.
[8] Lacabanne C, Goyaud P, Boyer RF. J Polym Sci 1980;18(3):277–84.
[9] Shrivastava K, Ranade JD, Srivastava AP. Thin Solid Films 1980;67(2):201–6.
[10] Mudarra M, Belana J, Cañadas JC, Diego JA. Polymer 1999;40(10):2659–65.
[11] Skinner SM, Svage RL, Rutzler Jr JE. J Appl Phys 1953;24(4):438–50.
[12] Skinner SM. J Appl Phys 1955;26(5):509–18.
[13] Possart W, Roder A. Phys Stat Sol A 1984;84(1):319–25.
[14] Derjaguin BV, Smilga VP. J Appl Phys 1967;38(12):4609–18.
[15] Lee L-H. Adhesive bonding. New York: Plenum, 1991.
[16] Dang C, Parpal J-L, Crine J-P. IEEE Trans Dielectr Electr Insul 1996;3(2):237–47.
[17] Hibma T, Zeller HR. J Appl Phys 1986;59(5):1614–20.
[18] Suh KS, Lee CR, Noh JS, Tanaka J, Damon DH. IEEE Trans Dielectr Electr Insul 1994;1(2):224–30.
[19] Crine JP. Phys Stat Sol 1982;72(a):789–97.
[20] Crine JP. IEEE Trans Dielectr Electr Insul 1997;4(5):487–95.
[21] Jonsson J, Ranby B, Mary D, Laurent C, Mayoux C. IEEE Trans Dielec Electr Insul 1995;2(1):107–13.
[22] Zhurkov SN, Zakresvskyi VA, Korsukov VE, Kuksenko VS. J Polym Sci 1972;10(A-2):1509–20.
[23] Popok VN, Odzhaev VB, Kozlov IP, Azarko II, Karpovich IA, Siridov DV. Nucl Instrum Meth Phys Res B 1997;129(1):60–64.
[24] Adamson AW. Physical chemistry of surfaces, 5. Wiley, 1990. p. 122.
[25] Nonnenmacher M, OBoyle MP, Wickramasinghe HK. Appl Phys Lett 1991;58(25):2921–3.
[26] Saurenbach F, Terris BD. Appl Phys Lett 1990;56(17):1703–5.
[27] Nyffenegger RM, Penner RM, Schierle R. Appl Phys Lett 1997;71(13):1878–80.
[28] Hong JW, Khim ZG, Hou AS, Park S. Appl Phys Lett 1996;69(19):2831–3.
[29] Terris BD, Stern JE, Rugar D, Mamin HJ. J Vac Sci Technol A-Vac Surf Films 1990;8(1):374–7.
[30] Cardoso AH, Leite CAP, Galembeck F. Langmuir 1998;14(12):3187–94.
[31] Cardoso AH, Leite CAP, Galembeck F. Langmuir 1999;15(13):4447–53.
[32] Martin Y, Williams CC, Wickramasinghe HK. J Appl Phys 1987;61(10):4723–9.
[33] Heinicke G. Tribochemistry. Berlin: Carl Hanser, 1984 (chap. 3).
[34] Livshits AI, Shluger AL, Rohl AL, Foster AS. Phys Rev B 1999;59(3):2436–48.
[35] Nunes SP, Costa RA, Barbosa SP, Almeida GR, Galembeck F. IEEE Trans Electr Insul 1989;24(1):99–105.